Precessionally-Driven Dynamo in a Spheroid

Cheng-Chin Wu and Paul H. Roberts
Institute of Geophysics and Planetary Physics
University of California, Los Angeles

Introduction

- More than a half century ago, Bullard conjectured that the motions necessary to generate the Earth's magnetic field in the Earth's electrically-conducting fluid core might be driven by the luni-solar precession.
- It has been unequivocally established in the intervening 55 years that precession can in principle supply the geodynamo with abundant power.
- The question of whether the geodynamo can draw on this power is still unanswered (though it seems probable from the work of Tilgner that it can do so).

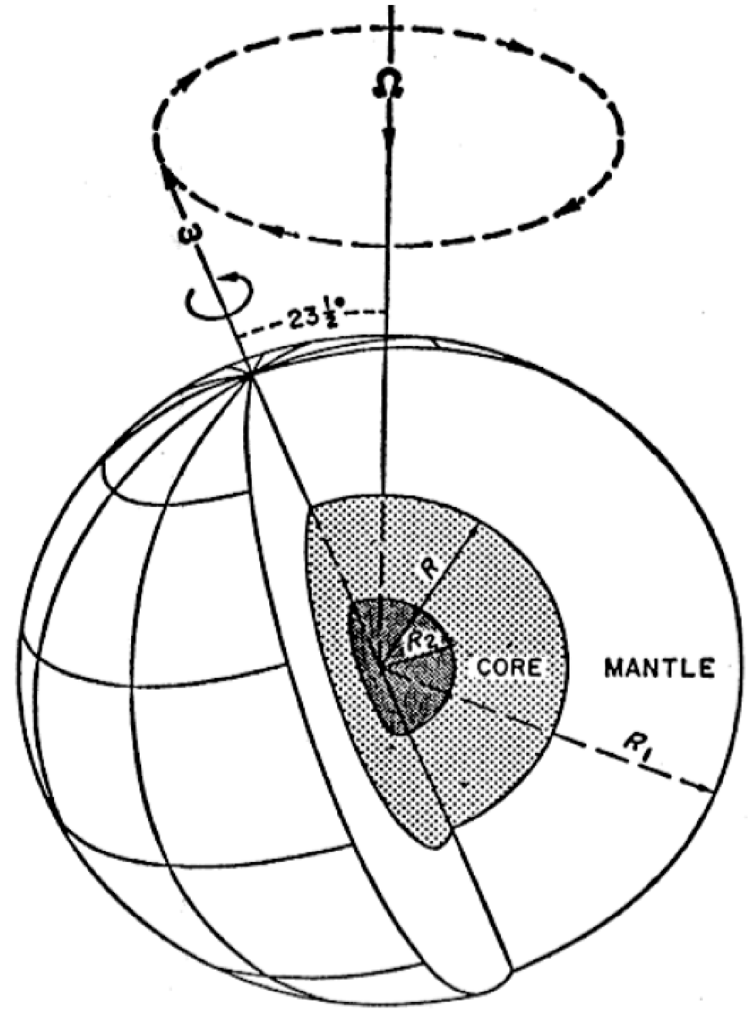

- Two types of precession-driven flows may be distinguished: in spherical precession, the mantle transmits motion to the core by viscous coupling; in non-spherical precession, the oblateness of the core-mantle boundary creates core motion through pressure differences.
- Non-spherical precession is being studied in a spheroid using a computer code for solving the time-dependent incompressible dissipative MHD equations with finite differences on overlapping grids. Here, the numerical methods and preliminary results are presented.
- We have studied the problem in a plane layer (Wu and Roberts, GAFD, 2008), where dynamo action is seen for strong precessional forcing.

Precessionally-Driven Fluid Model in a Spheroid

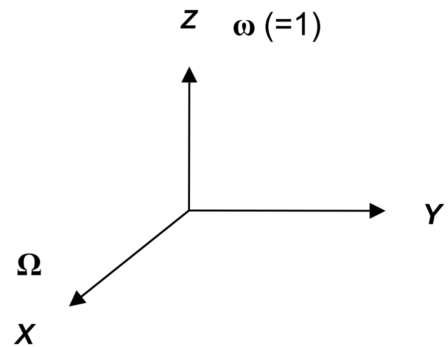

We consider the motion of a viscous fluid in a spheroidal container, which is rotating (rapidly) with angular velocity $\omega \hat{z}$ in a frame rotating (slowly) at angular velocity $\Omega \hat{x}$. In this **precessing frame**, $\boldsymbol{r} = x\hat{x} + y\hat{y} + z\hat{z}$; $\hat{x}$ $\hat{y}$ $\hat{z}$ are unit vectors.

Equations

The equations of motion are

$$\frac{\partial \mathbf{u}}{\partial t} + 2\Omega \hat{x} \times \mathbf{u} + \mathbf{u} \bullet \nabla \mathbf{u} + \nabla P = E \nabla^2 \mathbf{u} \qquad \nabla \bullet \mathbf{u} = 0$$

with the boundary conditions

$\mathbf{u} = \hat{z} \times \mathbf{r}$ on surface

where Ekman number E=ν/ωa^2, with a=semi-major radius (=1).

In the magnetic case, the equations are:

$$\frac{\partial \mathbf{u}}{\partial t} + 2\Omega \hat{x} \times \mathbf{u} + \nabla \bullet (\mathbf{uu} - \mathbf{BB}) + \nabla P = E \nabla^2 \mathbf{u}$$

$$\frac{\partial \mathbf{B}}{\partial t} + \nabla \bullet (\mathbf{uB} - \mathbf{Bu}) = E_{\mathrm{m}} \nabla^2 \mathbf{B}$$

$$\nabla \bullet \mathbf{u} = 0 \qquad \nabla \bullet \mathbf{B} = 0$$

subject to the boundary conditions, $\mathbf{u} = \hat{z} \times \mathbf{r}$ on the surface and **B** is connected to an external potential field determined by the continuity of **B** on the surface, and **B** →0 for |r| → ∞. Here E_m is the magnetic Ekman number, E_m=η/ωa^2, with η the magnetic diffusivity.

Basic Flow Solution in the Non-Magnetic Case

Poincaré's basic state in the **precessing frame** is

$$\mathbf{u}_{basic} = \begin{bmatrix} 0 & -1 & 0 \\ 1 & 0 & -(1+\varsigma)\mu \\ 0 & \mu & 0 \end{bmatrix} \mathbf{r}$$

where $\mu = 2\Omega/\zeta$ and ζ is defined by the equation for the surface of the spheroid:

$$x^2+y^2+(z/c)^2=x^2+y^2+(1+\zeta)\, z^2=1$$

As in Kerswell [The instability of precessing flow, GAFD, 72, 107, 1993], we solve the flow equations in terms of the deviation of the flow solution from the basic state:

$$\tilde{\mathbf{u}}=\mathbf{u}-\mathbf{u}_{\text{basic}}$$

subject to the stress-free boundary conditions for **ũ.**

(For the Earth, $\Omega \sim 4\text{x}10^{-8}$, $\zeta \sim 1/200$.)

Numerical Method

The set of equations can be written in the form:

$$\frac{\partial \mathbf{u}}{\partial t} + \nabla P = RHS$$

$$\nabla \bullet \mathbf{u} = 0$$

A 2nd order Runge-Kutta scheme is used in the time-integration. For each Runge-Kutta stage, a fractional-step method [Kim & Moin, 1985] is used:

(1) Solve $\partial \mathbf{u}^*/\partial t = RHS$ from $t=t_n$ to $t_n+\Delta t$ and obtain $\mathbf{u}^*$,

(2) Solve $\nabla^2 p = \nabla \bullet \mathbf{u}^*$ to obtain p,

(3) Set $\mathbf{u}(t_n+\Delta t) = \mathbf{u}^* - \nabla p$.

The quantity *RHS* is evaluated using 2nd order accurate central finite differences.

Numerical stability is provided by explicit dissipation terms.

Overlapping Grids

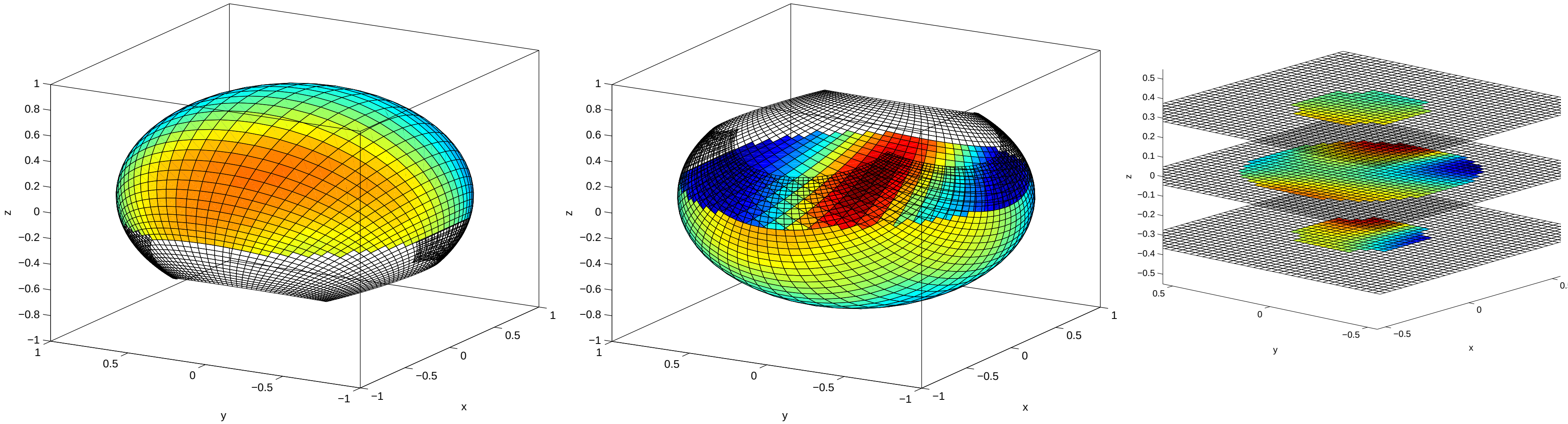

To cope with the condition imposed by the geometry of container, a method of overlapping grids is used; see the software package “Overture”, developed by Henshaw and his team at LLNL.

In the implementation for the spheroidal container, three grids are used: two spheroidal-shell grids and a 3D rectangular grid. The shell grids overlap each other as depicted above. The rectangular grid fills the inner region and overlaps with the outer two shell grids. These grids not only solve the geometry problem of the container, but also avoid the grid singularities (so-called pole problems), where the time-step size could be extremely limited due to the CFL condition.

Poisson Solver

Following Lai, Lin, and Wang [2002], a FFT-based fast direct solver for the Poisson equation $\nabla^2 p = \nabla \bullet \mathbf{u}^*$ in spheroidal geometry is developed. In spheroidal coordinates μυθ, we approximate the solution by truncated Fourier series in θ. The resulting equations for the Fourier coefficients as functions of μ and υ are then solved using the cyclic reduction method [Buneman, 1969]. A routine in Fishpack [Adams, Swarztrauber, & Sweet, 1980] was used in our work.

This 4th grid of spheroidal coordinates is overlapped with the other 3 grids.

Computational Costs

Poisson solver: NLM log(M); NLM: number of grid points in $\mu\upsilon\theta$ directions
Other operations: NLM (NLM: number of grid points in the 3-grid system)
(For calculations shown later, the Poisson solver represents about 1/3 of the cost.)

The method can be adapted to parallel clusters.

The method can be used for a sphere. The cost is of the same order for a sphere as for a spheroid.

Code Validation

(1) Solutions of the magnetic diffusion equation in spheres and spheroids.

(a)The longest-lived magnetic decay mode (the gravest mode) for a sphere is found numerically to be within 1% of the analytical decay rate.

(b) Numerical values of the decay rates for the gravest poloidal and toroidal decay modes of a spheroid are found to be in good agreement with values obtained by a completely separate program which makes use of the properties of the spheroidal wave functions

(2) Kinematic dynamos in spheres:

The marginal values of the magnetic Reynolds number are found to be consistent with results for kinematic dynamos models of (a) Dudley and James (1989), model 2; (b) Lilley (1970), as modified by Gubbins (1973); and (c) Kumar & Roberts (1975); see also Love & Gubbins (1996), Sarson & Gubbins (1996), and Gubbins *et al.*, (2000a,b).

Numerical Results

- linear instability of the Poincaré's flow
- nonlinear flow motions in a spheroid
- kinematic dynamo of precessionally forced motions
- full nonlinear precessionally-driven dynamo problem.
- Parameters: c, ratio of minor/major radii is 0.8; and Ω is ¼.

[For *E*=0, Kerswell (1993) has obtained exact linear solutions.
For quadratic velocities, he found instability in a region
c < approximately 0.85.]

Non-magnetic calculations:
Linear growth

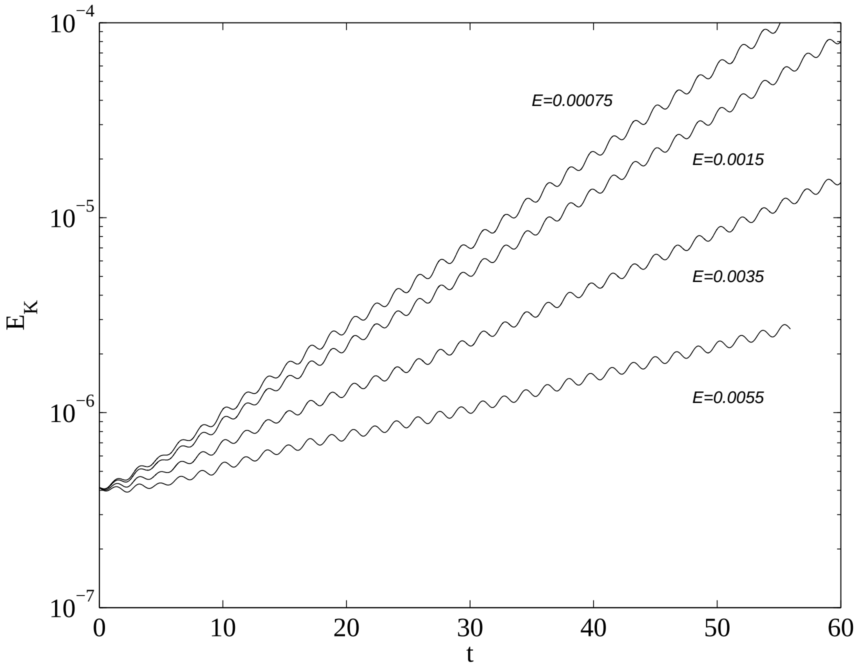

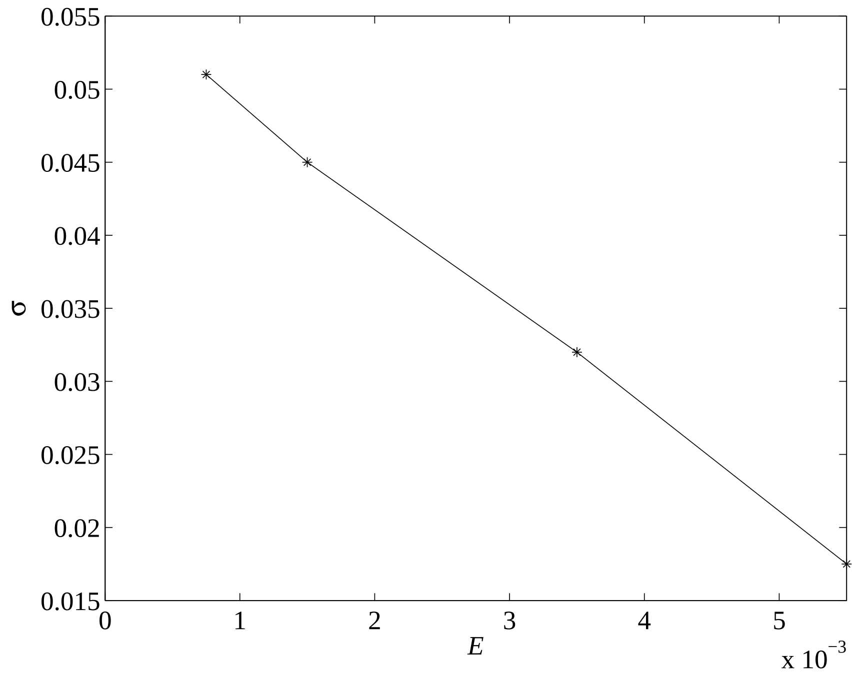

Kinetic energy vs t for calculations with several Ekman numbers for the case with c=0.8 and Ω=0.25. (Inner grid: 513 points; outer shells: 71x71x61 points each.)

Linear growth rate vs Ekman number for the case with c=0.8 and Ω=0.25. Theoretical value of σ at *E*=0 is 0.054 (Kerswell, 1993).

$\widetilde{u}$ at t=0 is given by the theoretical eigenvectors for the case *E*=0.

E_K=sum of $\widetilde{u}^2$ over each grid points; no geometric factor is inculded.

Non-magnetic calculations:
nonlinear solution (1)

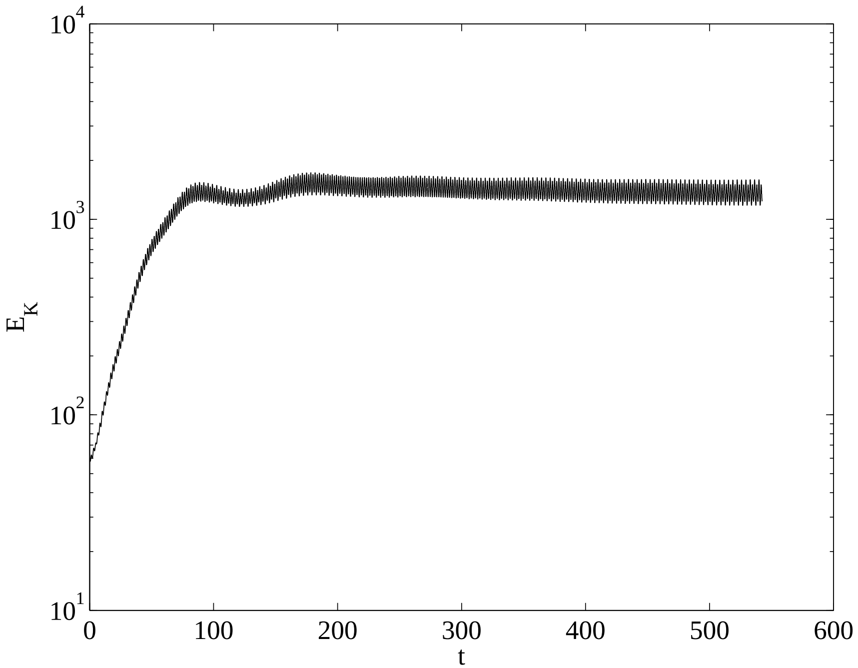

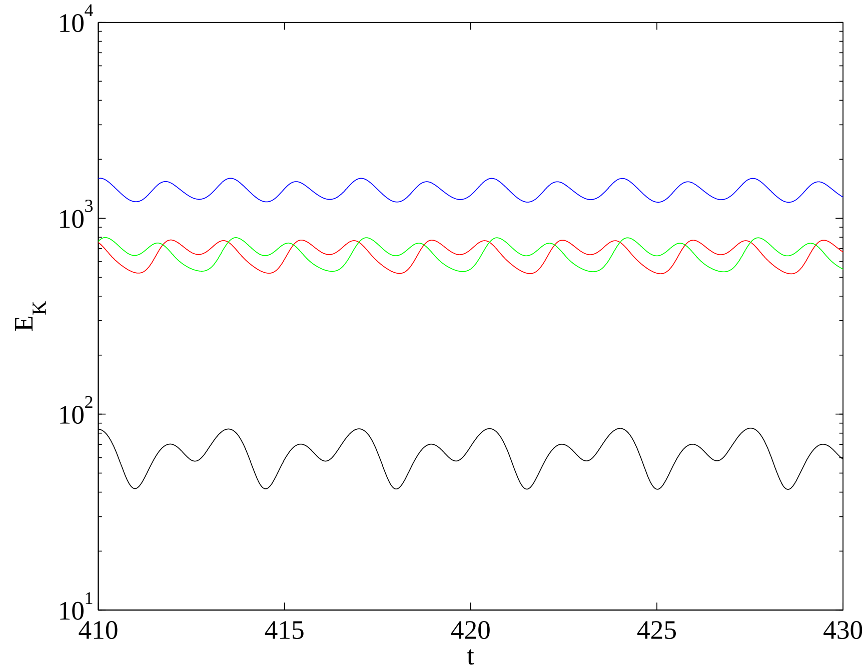

Kinetic energy vs t for the case with *E*=0.0035, c=0.8 and Ω=0.25.

Blue: total
Red: top shell
Green: bottom shell
Black: inner grid

Non-magnetic calculations: nonlinear solution (2)

Flow ($\widetilde{u}$) at t=411; Vector plots on the surface

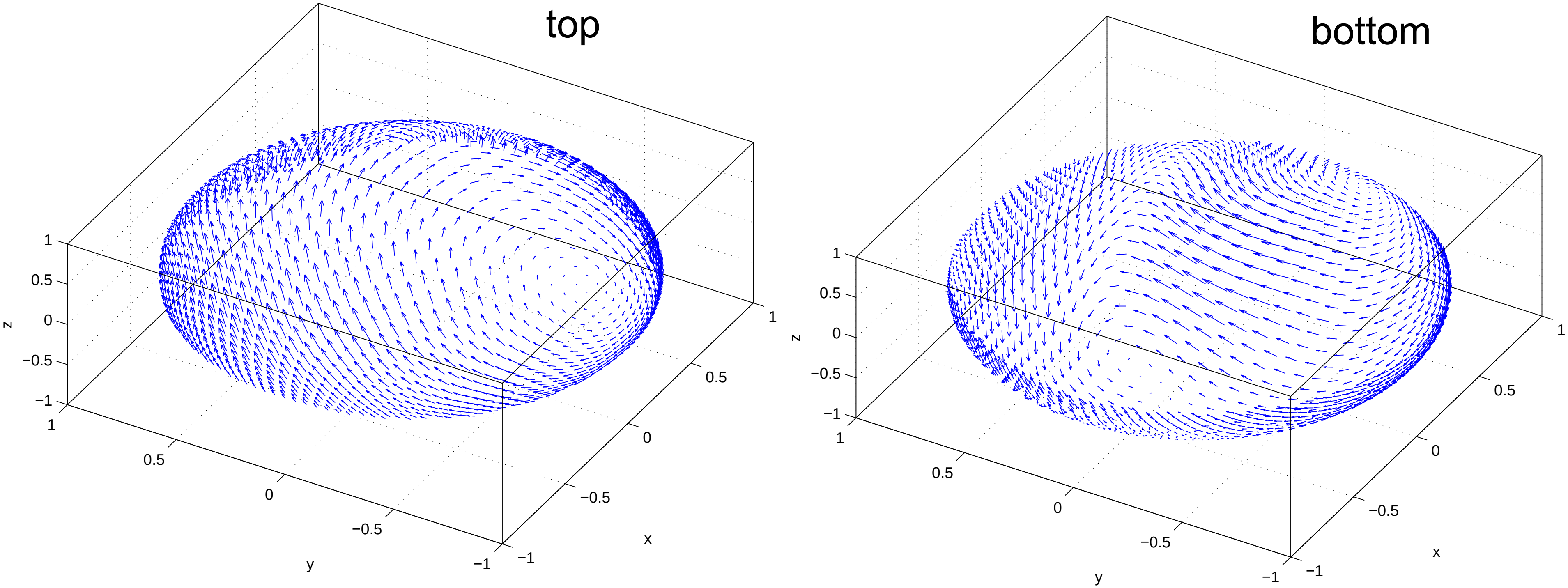

Non-magnetic calculations: nonlinear solution (3)

Flow ($\widetilde{u}$) at t=411

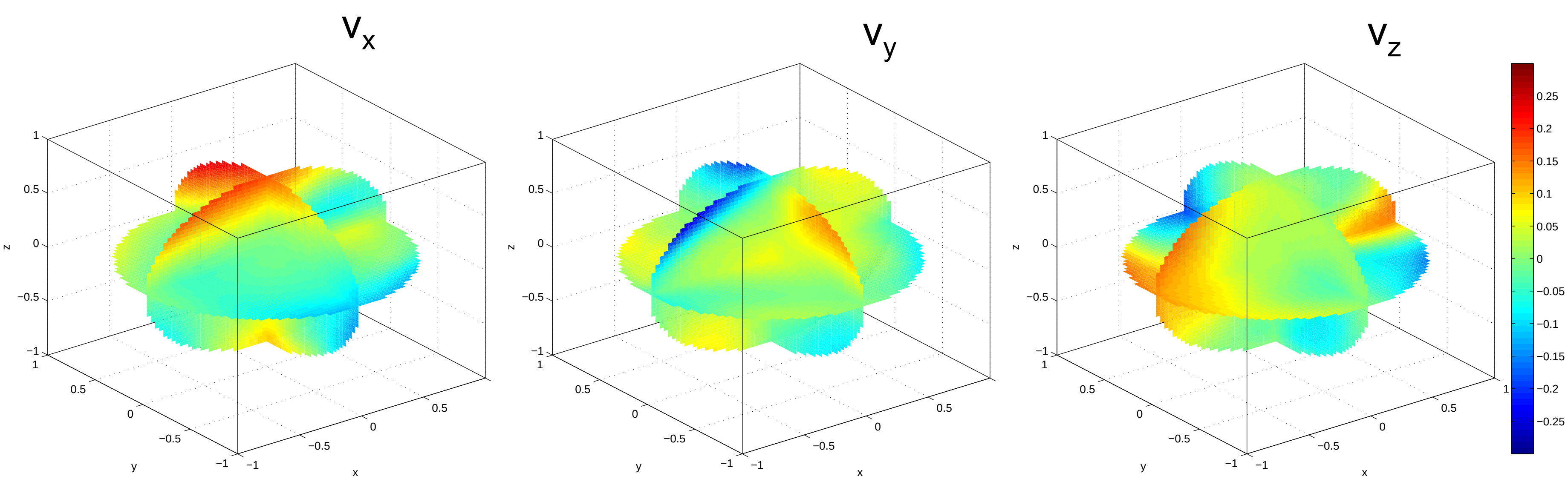

Non-magnetic calculations: nonlinear solution (4)
A second example

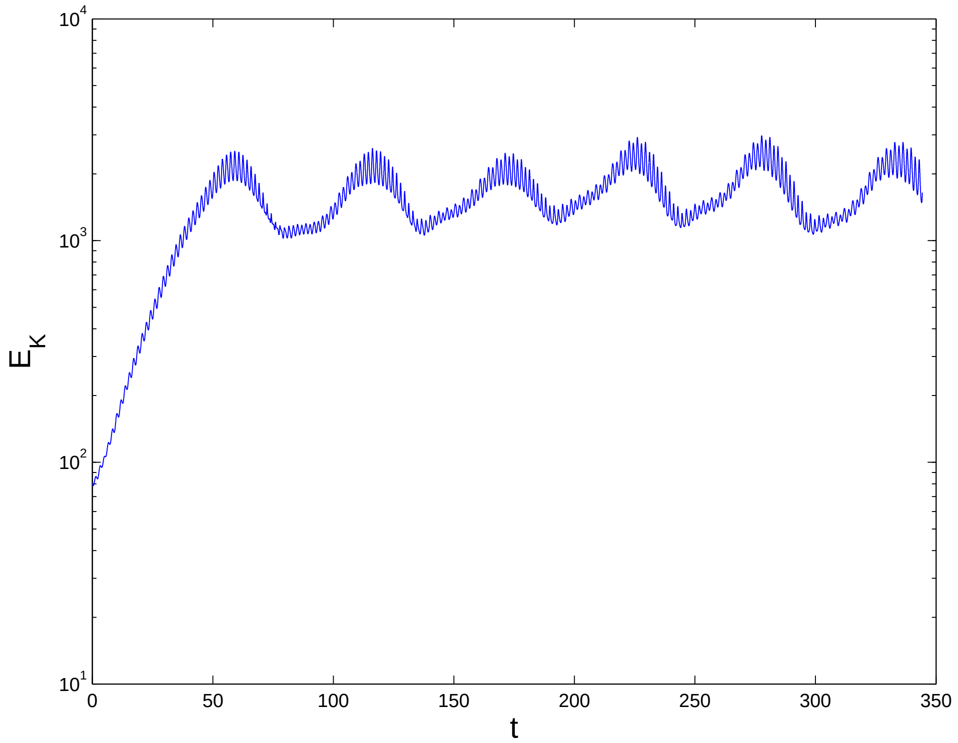

Kinetic energy vs t for the case with *E*=0.0011, c=0.8 and Ω=0.25. (Inner grid: 51^3 points; outer shells: 83x83x61 points each.)

Kinematic dynamo calculations (1)

For the case with E=0.0035, c=0.8 and Ω=0.25.

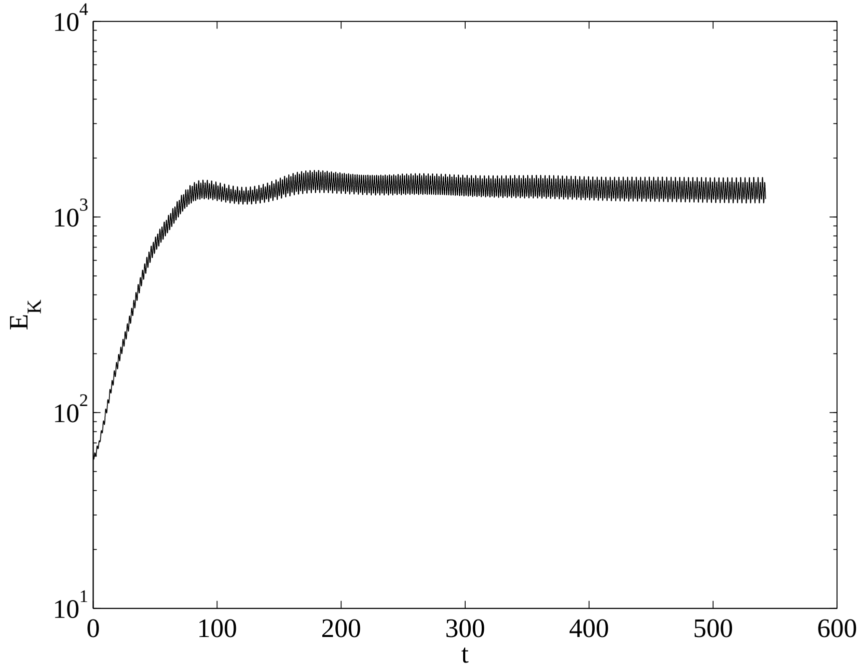

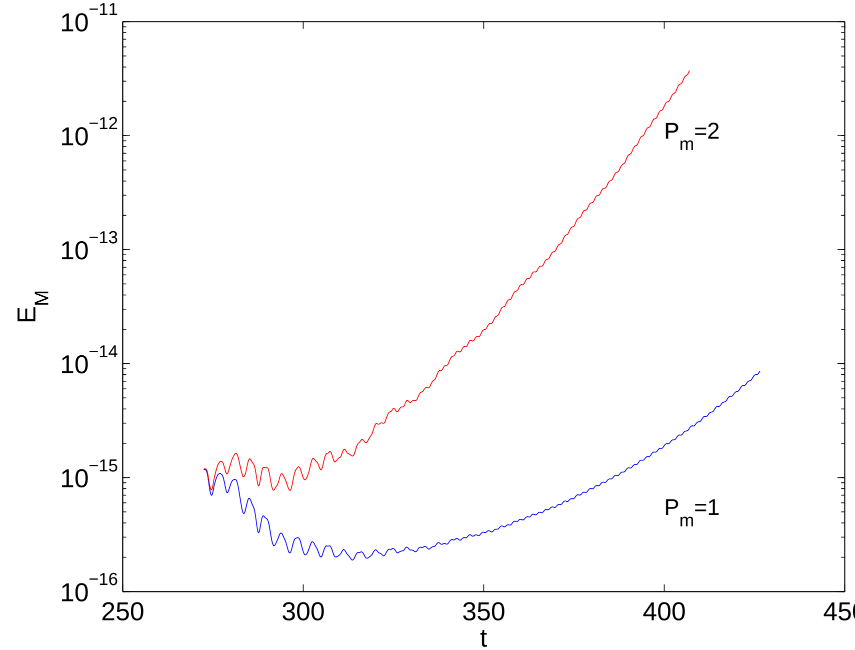

Small magnetic field is added at t=272.
Right panel: Kinetic energy vs t
Left panel: Plots of magnetic energy vs t for
Prandtl number $P_m = E/E_m$ = 1, and 2.

Full MHD calculations (1)

For the case with E=0.0035, P_m=2, c=0.8 and Ω=0.25.

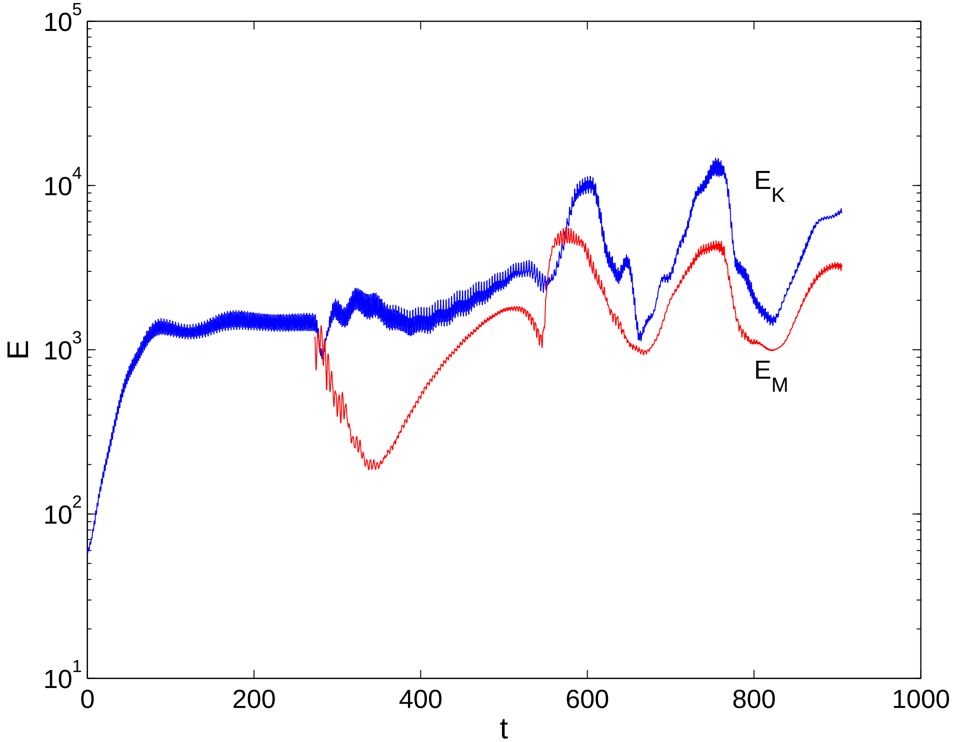

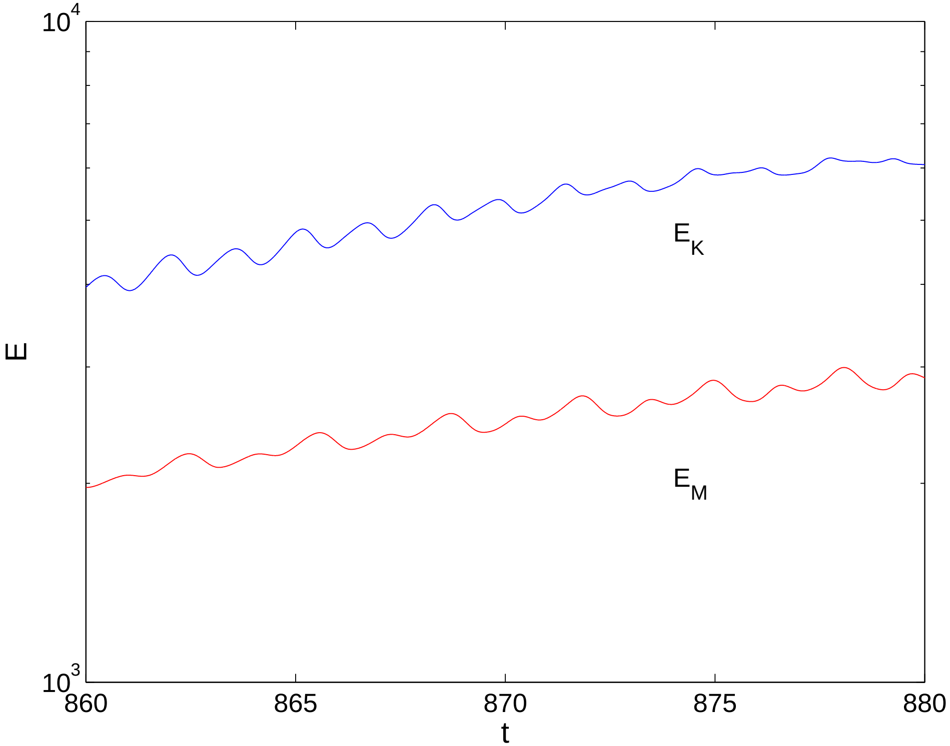

Magnetic field is added at t~272.

Full MHD calculations (2)

V and B at $t=871.3$ for the case with $E=0.0035$, $P_m=2$, $c=0.8$ and $\Omega=0.25$.

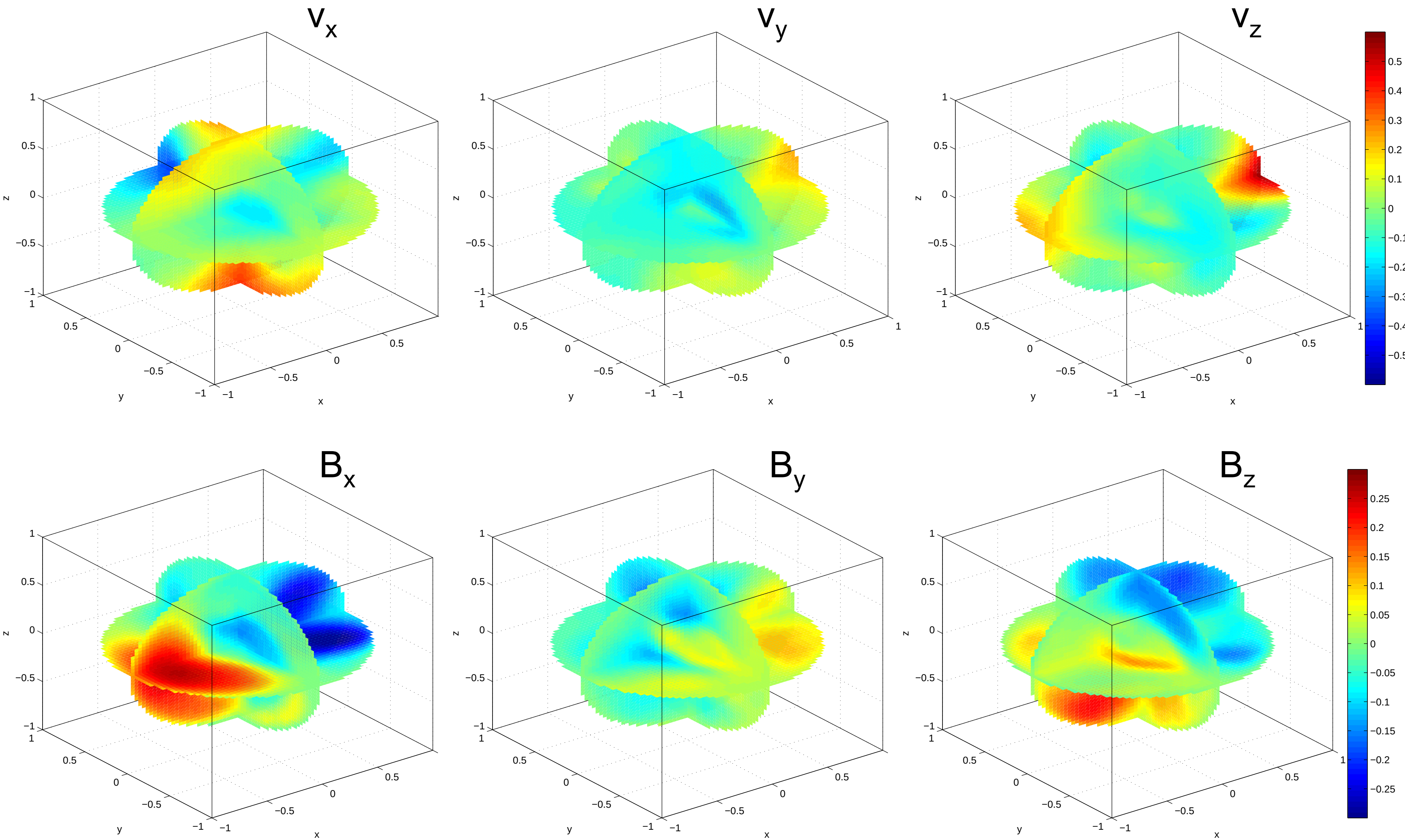

Full MHD calculations (3)

For the case with E=0.002, P_m=*0.5*, c=0.8 and Ω=0.25.

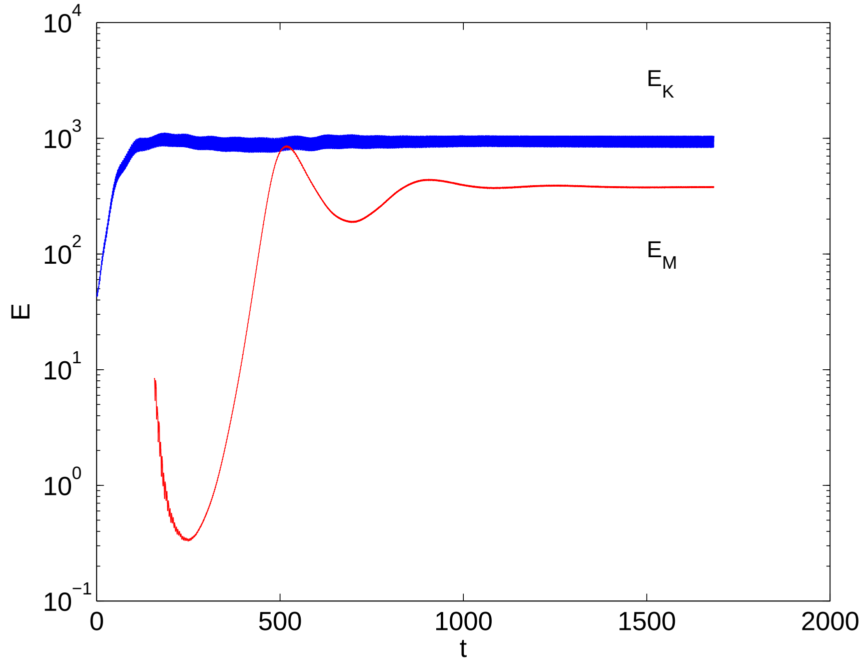

Magnetic field is added at t~160.

Conclusions / The future

- It appears that the numerical method that has been selected provides a practical way for studying both non-magnetic and magnetic precessionally-driven flows in both spheres and spheroids. The preliminary results indicate that precessionally forced motions can maintain magnetic fields by dynamo action. Nevertheless, much remains to be done. More cases, as function of c, Ω, E and E_m, need to be studied.
- To achieve small Ekman numbers, a high order accurate code such as the WENO code (Wu, 2007) would be used. It has the additional advantage of being numerical stable even when there are no explicit dissipation terms in the equations.
- Also, the code should be parallelized to utilize the power of a cluster of computers.
- There are many longer term objectives too, e.g., (1) To bring the system closer to the real Earth, it is desirable to generalize the present approach by adding a solid inner core. (2) It would be interesting to know whether the convective dynamos that are currently being studied all over the world are significantly affected when precessional forcing is included.